



Solar biomass pyrolysis for the production of bio-fuels and chemical commodities

Sergio Morales^a, Rosa Miranda^{a,b,*}, Diana Bustos^a, Thania Cazares^a, Honghi Tran^b

^a Universidad Autónoma de Nuevo León, Facultad de Ciencias Químicas, Chemical Engineering Department, Universidad Ave. S/N, Ciudad Universitaria, San Nicolás de los Garza, 66450 Nuevo León, Mexico

^b Pulp & Paper Centre, Chemical Engineering and Applied Chemistry, University of Toronto, 200 College Street, M5S 3E5 Toronto, Ontario, Canada

ARTICLE INFO

Article history:

Received 24 February 2014

Accepted 20 July 2014

Available online 4 August 2014

Keywords:

Solar biomass pyrolysis

Bio-fuel

Solar reactor

Ray-tracing method

Heat balance

Parabolic-trough concentrator

ABSTRACT

This study investigated orange-peel pyrolysis due to solar radiation that was applied as a unique source of energy using a parabolic-trough solar concentrator. An optical analysis was conducted using a Monte Carlo ray-tracing method to provide a detailed tridimensional description of the optical performance of the thermo-solar system. The average irradiance of the pyrolytic reactor surface was 15.65 suns. The peak irradiance was very similar to that calculated using the ray-tracing method, confirming that the operational conditions were optimal. The heat balance was analyzed by applying optical and thermodynamic principles. The main heat losses were caused by the reflectivity of the biomass (37.85%) and the difference between the temperatures of the environment and the reactor (36.23%). The solar pyrolytic reactor reached a peak temperature of 465 °C at the middle of the focal line. The total weight loss of the orange peels was 79 wt.% at an average irradiance of 12.55 kW/m². Furthermore, substances valuable to the energy, chemical and pharmaceutical industries were identified in the bio-oil that was produced during solar pyrolysis, such as (Z)-9-octadecenamide, diisooctyl phthalate, squalene, D-limonene, and phenol.

© 2014 Elsevier B.V. All rights reserved.

1. Introduction

One of the most complex challenges that humanity must face today is managing and halting the climate change produced by the over-exploitation of natural resources. On October 31st, 2011, the global human population included 7 billion inhabitants and it is forecasted to reach 9.3 billion by 2050 [1]. This forewarned large population will surely increase the demand for energetic resources. The use of thermo-solar energy and the production of bio-fuels using biomasses are options that may offer a sustainable solution to the energy needs of the modern human being without compromising the environment.

The two main types of processes that can convert biomasses into useful bio-fuels are thermochemical and biochemical processes. The thermochemical processes include gasification, pyrolysis, liquefaction and combustion [2]. The biochemical processes have

conversion efficiencies of between 35 and 50 wt.%, whereas the thermochemical processes have conversion efficiencies of 41–77 wt.% [3]. In addition to transforming the biomass into bioenergetics, these processes can be used to produce almost any product of the petrochemical industry [2]. One of the thermochemical processes with the highest flexibility in terms of the yield and composition of the products that can be obtained is pyrolysis. Pyrolysis of a biomass is defined as the thermal degradation of the biopolymers present in the organic material under an inert oxygen-free atmosphere [4]. This process can be used to produce bio-fuels, bio-oils, biogas and chars in various proportions depending on the type of pyrolysis, the selected reactor and the operational conditions. An advantage of pyrolysis is that it can convert over 60 wt.% of the biomass into a liquid bio-oil [4,5]. However, pyrolysis has the disadvantage of requiring an external energy input to reach the operating temperature, which may range from 300 °C to 650 °C, to promote the formation of liquid products [2]. This external energy input is generally derived from a non-renewable source that has a negative impact on the environment. A possible solution to this problem is to use thermo-solar energy to heat the reactor to obtain solar pyrolysis.

Solar biomass pyrolysis is an endothermic process of converting a biomass in an inert atmosphere in which the required heat

* Corresponding author at: Pulp and Paper Centre, Chemical Engineering and Applied Chemistry, University of Toronto, 200 College Street, M5S 3E5, Toronto, Ontario, Canada. Tel.: +1 4 1694 67556.

E-mail addresses: rosymirandag@yahoo.com.mx, rosa.miranda@utoronto.ca, rosymirandag@hotmail.com (R. Miranda).

Nomenclature

I	insolation, W/m ² . Eq. (5)
q_0	concentrated radiation, W/m ² . Eqs. (3) and (4)
c	circumference, m. Eq. (5)
$Q_{\text{absorbed}}^{\text{solar}}$	absorbed solar energy by the thermo-solar system, J. Eqs. (2) and (3).
Q_{reactor}	heat in the reactor, J. Eqs. (2) and (6)
Q_{biomass}	heat in the biomass, J. Eqs. (2) and (7)
$Q_{\text{loss to the environment}}$	environmental heat loss, J. Eqs. (2) and (8)
Q_{rxn}	reaction heat of the pyrolysis, J. Eqs. (2) and (10)
α_{reactor}	absorbance of the reactor, fraction. Eq. (3)
α_{biomass}	absorbance of the biomass, fraction. Eq. (3)
τ_{reactor}	transmittance of the reactor, fraction. Eq. (3)
η_{optic}	optic efficiency, %. Eq. (4)
η_{focus}	focusing efficiency, %. Eq. (4)
A	surface area of the reactor, m ² . Eqs. (4) and (8)
t	residence time of the biomass, s. Eqs. (4) and (8)
φ	irradiance across the circumference of the reactor, W/m ² , Eqs. (4) and (5)
T_{∞}	environmental temperature, °C. Eqs. (6)–(8)
T_f	operational temperature, °C. Eqs. (6)–(9)
M_{reactor}	mass of the reactor, kg. Eq. (6).
M_{biomass}	mass of the biomass, kg. Eqs. (7) and (10)
$C_{p \text{ reactor}}$	heat capacity of reactor, J/kg °C. Eq. (6)
$C_{p \text{ biomass}}$	dried orange peel heat capacity, J/kg °C. Eq. (7)
h	heat loss coefficient (convection and radiation to the environment), W/m ² °C. Eqs. (8) and (9)
H_{rxn}	enthalpy of the orange peel pyrolysis per mass unit, J/kg. Eq. (10)
L	Length of the reactor, m
Φ	Diameter of the reactor, in.
FC	Fixed carbon, wt.%

is provided by concentrated solar energy. The direct solar insolation is concentrated and redirected to the pyrolytic reactor by an optical system. This concentrated energy allows the reactor and the biomass to reach pyrolytic temperatures. There are three possible ways to transfer the solar heat to the biomass, as follows: through the walls of the reactor, by applying direct irradiation of the carbonaceous material or by employing an intermediate heat-carrying fluid [6]. When the biomass is directly irradiated, the biomass will become the hottest portion of the system and the reactor will remain at a lower temperature, reducing the rate of secondary decomposition reactions in the gas phase.

Solar biomass pyrolysis may be performed using a thermo-solar system. A thermo-solar system concentrates and redirects the solar radiation from a large area into a smaller one to use this energy as a heating source. Thermo-solar systems consist of 3 main parts, which are the solar concentrator, the solar collector, and a supporting structure. The solar concentrator focalized the solar radiation on the surface of the solar collector, which in this study was a tubular pyrolytic reactor. Both components were mounted on the supporting structure. A summary of the different types of solar concentrators is shown in Table 1. Because a parabolic-trough concentrator produces a focal line of radiation, this apparatus is the ideal option for heating tubular reactors to the temperatures needed for biomass pyrolysis.

The pyrolysis of carbonaceous materials using concentrated radiation has been studied by a few authors (Table 2). The mass loss reported by the authors ranged from 20 to 92 wt.% upon concentrated irradiation. However, most of the studies used coal or cellulose as the raw material and the yields of pyrolytic liquids or main compounds were not reported. Tabatabaie-raissi et al.

[16] and Boutin et al. [17,18], who performed cellulose pyrolysis using concentrated radiation emitted by a xenon lamp, obtained a mass loss of 92.1 wt.% and 20.0 wt.%, respectively. Boutin et al. [18] concluded that the relatively low mass loss observed was due the shrinkage of the cellulose that occurred during thermal degradation moving the sample out of the focal point. Beattie et al. [19] pyrolyzed a coal sample using concentrated solar energy. The authors found that pyrolysis of the coal occurred when the irradiation level was greater than 200 W/cm², which resulted in 51 wt.% of volatiles and no tar formation. To date, there is scarce information in the literature regarding solar pyrolysis and even less information involving solar pyrolysis of agro industrial waste.

To date, a small number of patents related to solar thermal conversion of biomasses into a bio-fuel have been filed. Most of the related research has focused on the production of hydrogen and carbon monoxide using natural solar radiation. The types of furnaces used include a solar-pump laser, a hybrid solar-syngas system and a solar/microwave system [20–22]. The solar radiation used for these processes has been augmented by conventional heating sources, such as microwaves and plasma; only McAllister [25] and Storey et al. [23] used solar thermal energy as the only heating source for a solar concentrator equipped with actuators [25] or with parabolic mirrors controlled via electric motors [23]. The raw materials generally used range from sisal residues [23], oil shale [24], biomasses, domestic waste, sludge from waste water, fossil coal [24,25] to pure cellulose [20]. The products of the solar processes included fuels [22], olefins and carbon, oil fines [21], H₂ [20,21,25,26], CO₂ [20,21] and vapor, the latter of which was used as a power source [21]. Further analysis of the optics, yields and description of the products of the solar systems has yet to be reported.

The solar production of bio-fuels offers a possible solution for storing solar energy in a chemical compound. Considering that a high-temperature process is used to induce an endothermic reaction in a solar chemical reactor, when energetic products are needed, an exothermic reaction would expel heat in an amount equal to the sum of the energy stored during solar thermal decomposition and photosynthesis [27,28]. This phenomenon allows exploitation of the energy stored in the compound at any place and at any time, even when the solar resource is not available (for instance, during the night or on cloudy days).

The direct use of solar radiation to induce pyrolysis has an advantage over traditional methods in that the process does not require the consumption of fossil fuels or electricity to bring the system to a pyrolytic temperature. Solar pyrolysis is a sustainable solution for the production of biofuels from agro-industrial wastes in cities with a high degree of insolation, such as Monterrey Mexico, which receives approximately 2245 kWh/m²a of sunlight [29].







Citrus fruits are the most abundant crops in the world, with more than 120 million tons/year of oranges, lemons, grapefruits and mandarins produced [30]. In 2010, Mexico produced 4 million tons of orange, of which 40 wt.% (approximately 1.6 million tons) became wet-solid residues of the orange industry [31].

The aim of the present study was to perform optical and thermal analyses of the process of producing a bio-fuel using solar pyrolysis of orange peels. In addition, the bio-oil was characterized. Because orange peels are an agro-industrial waste with a negative impact on the environment, the present project addressed to the need to identify new renewable energy sources and demonstrated a possible approach to solid agro-industrial waste management.

2. Methodology

The methodology of this study involved the eight following steps: sample preparation, sample characterization, solar

Table 1
Types of solar concentrators and their main characteristics.

Concentrator	Diagram	Reflective material	Focal type	Operating temperature (°C)	Characteristics	Reference
Parabolic dish		Mirror	Focal point	1200	Difficult to build. Uses only direct solar radiation A 2-axis tracking system can be used	Pfänder et al. [7], Luzzi and Lovegrove [8], Leitner [9]
Heliostat		Mirror	Focal point	900	Multiple heliostats are required to reach the maximum temperature. Easy to build Uses only direct solar radiation. A 2-axis tracking system can be used	Luzzi and Lovegrove [8], Adinberg et al. [10], Leitner [9]
Parabolic-trough		Mirror	Focal line	400	Ideal for heating cylindrical surfaces. Uses only direct solar radiation A 1-axis tracking system can be used	Luzzi and Lovegrove [8], Fernández-García et al. [11], Leitner [9]
Compound parabolic		Mirror	Focal line	150	Ideal for low temperature processes Can focus direct and diffuse solar radiation A 1-axis tracking system can be used	Luzzi and Lovegrove [8], Xuan et al. [12], Guiqiang et al. [13]
Linear Fresnel		Mirror	Focal line	350	Easy to build. Uses only direct solar radiation A 1-axis tracking system can be used	Luzzi and Lovegrove [8] Velazquez et al. [14]
Fresnel lens		Glass	Focal point	350	Fragile and expensive. Uses only direct solar radiation A 2-axis tracking system can be used	Xuan et al. [12], Rändler [15]

pyrolysis, optical analysis of the system, solar pyrolysis of the biomass, bio-oil characterization, mass balance and heat balance, which are described below.

2.1. Sample preparation

The biomass used for solar pyrolysis was orange peel (*Citrus sinensis*), obtained from an orange-juice production company located in Monterrey, Mexico.

The orange peels were dried for 5 hours in a wind tunnel powered by a 1-hp blower, under standard conditions of temperature and pressure. The dry orange peels were shredded into two average particle sizes of 20 mm × 20 mm × 3 mm (Experiment 1) and 30 mm × 3 mm × 3 mm (Experiment 2). Each particle-size sample was used in separate experiments and the batches of different particle size were never mixed.

2.2. Sample characterization

To determine the chemical composition of the orange peels, elemental and proximate analyses were conducted. Proximate analysis of the samples was performed according to ASTM method D3172. The elemental analysis was performed in a Perkin Elmer

2400 (CHNOS) analyzer using ASTM method D-5373. The oxygen content was calculated from the difference.

The thermogravimetric analysis of the sample was performed using a model Q500 TA instrument. The analysis was conducted using a powdered (containing 450-μm particles) sample (~10 mg) while maintaining a constant nitrogen-flow rate (100 ml/min). All of the experiments were conducted in the temperature range of 25–800 °C at five different heating rates, 1, 5, 10, 20 and 40 °C/min.

2.3. Solar pyrolysis system

A system for solar pyrolysis was designed and constructed by combining a concentrated radiation system with a thermochemical biomass conversion system. Relatively few solar pyrolytic systems have been experimentally tested, and if so, the tests were generally performed at laboratory scale. These studies were conducted mainly for gasification and not for pyrolysis. The solar pyrolysis system consisted of 3 elements: the solar reactor, the hub, and the condensation train, as proposed by Miranda et al. [32] and Morales [33]. A detailed description of the design and construction of the solar pyrolysis system was previously provided [32]. A tubular reactor composed of borosilicate glass, of 2 in of diameter and 16 in length with a transmittance rate of 0.92, was used with

Table 2
Pyrolysis of carbonaceous materials subjected to concentrated radiation.

Raw material	Heating source	Radiation concentrator	Reactor Shape	Material	Dimensions	Mass loss (wt.%)	Char (wt.%)	Reference
Avicel microcrystalline cellulose PH105	Xenon lamp	2 parabolic concentrators	Cylindrical	Molten silica	Ø 1.38 × 25.20 in.	92.1	7.9	Tabatabaie-raissi et al. [16]
Arizona Southwest Coal	Sun	1 heliostat and 1 parabolic Concentrator	Dome-like cylindrical with a quartz window	Molten silica and steel	399 cm ³	51	49	Beattie et al. [19]
Whatman cellulose pellets	Xenon lamp	2 parabolic concentrators	Cylindrical	Molten silica	Ø 1.18 in. × 1.97 in.	20	80	Boutin et al. [17]
Whatman microgranular CC31 cellulose	Xenon lamp	2 elliptical mirrors and a diaphragm with pendulum	Spherical	Borosilicate glass	Ø 0.20–0.24 in.	^a	^a	Boutin et al. [18]

^a Data not reported.

helium as the carrier gas. The borosilicate glass allowed most of the concentrated irradiation to pass through the walls of the reactor due to its having a transmittance level (92%) similar to that of quartz (94%) but a lower cost. The high transmittance of the reactor material allowed the biomass to be heated directly. As a result, the biomass was the hottest material in the system because it absorbed the most solar irradiation. A parabolic-trough concentrator was designed and built. The parabolic curvature was given by the equation $Z = x^2/4f$, where f represents the position of the focal line with respect to the vertex of the parabola. The surface of the concentrator was covered with a silver-mirror coating to reflect and concentrate the solar radiation. This type of concentrator has the advantage of focusing the solar energy in a straight line, so that the parabolic trough concentrator and the tubular reactor caused heating of majority of the biomass. The solar concentration system consisted of a silver mirror-coated parabolic-trough concentrator with a 1300-mm-wide aperture (Fig. 1). The silver reflective surface that was deposited over the 6-mm-thick glass had a reflectance of 0.94, absorbance of 0.06, transmittance of 0.00 and a specular standard deviation of 0.5 mrad. The hub was the metallic supporting structure for the concentrator and the reactor, which could rotate in one axis to re-focus the system throughout the day.

2.4. Optical analysis of the system

An optical analysis performed to evaluate the irradiance profile of the solar reactor. The optical analysis was based on the Monte Carlo ray-tracing method. The ray traces were calculated using the SolTrace software that was developed by the National Renewable Energy Laboratory (NREL). Ray tracing was achieved using an insolation of 1 sun and was discretized in a Gaussian distribution of 100,000 vectors. The thermo-solar system was divided in two stages. The first one was the reflective surface of the parabolic-trough solar concentrator, which had the following characteristics: aperture width of 1.3 m, transmittance of 0.00, reflectivity of 0.94, absorbance of 0.06 and a specular standard deviation of 0.5 mrad (Fig. 1). The second stage was the surface of the tubular borosilicate-glass reactor, which had an external diameter of 2 in. Optical analysis was used to determine the path of the solar rays in the system so the irradiance profile of the outer surface of the solar reactor could be calculated.

2.5. Solar pyrolysis of the biomass

The following steps were performed to conduct solar biomass pyrolysis: first, the biomass was introduced into the tubular reactor and then the reactor was mounted in the focal line of the solar concentrator. Then, the solar concentrator was focalized according to the angle of the sunlight and the nitrogen flow was begun to produce an inert atmosphere. Subsequently, the temperature began rising to reach a pyrolytic temperature, and the gases that were generated during solar pyrolysis were transferred to a condensation-train system consisting of 3 cooling traps immersed in liquid nitrogen at -200°C at the atmospheric pressure. The incondensable gases were passed through a wet scrubber. The last steps of the process were to cool the reactor to the environmental temperature and to collect the solid and liquid products. Fig. 2 shows a flow chart of the experimental process.

The system concentrated the sunlight on a small area of the reactor and the biomass captured that radiative energy via the concentrator–reactor system. The biomass absorbed a portion of the concentrated irradiation, increasing its temperature and allowing thermal decomposition to occur.

During the solar biomass pyrolytic process, the insolation (I) was measured using at ground level using a pyranometer, whereas a concentrated-radiation sensor measured the concentrated

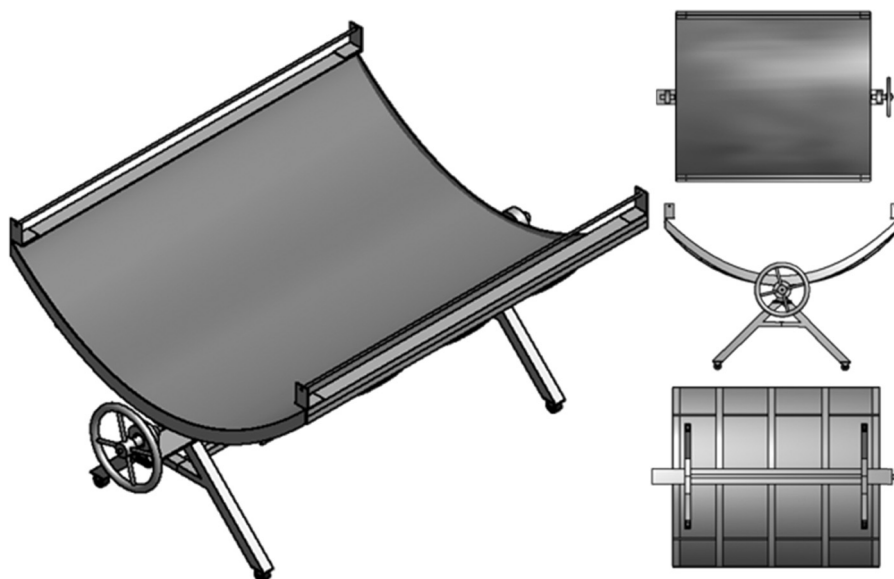


Fig. 1. Parabolic-trough solar concentrator used for solar pyrolysis.

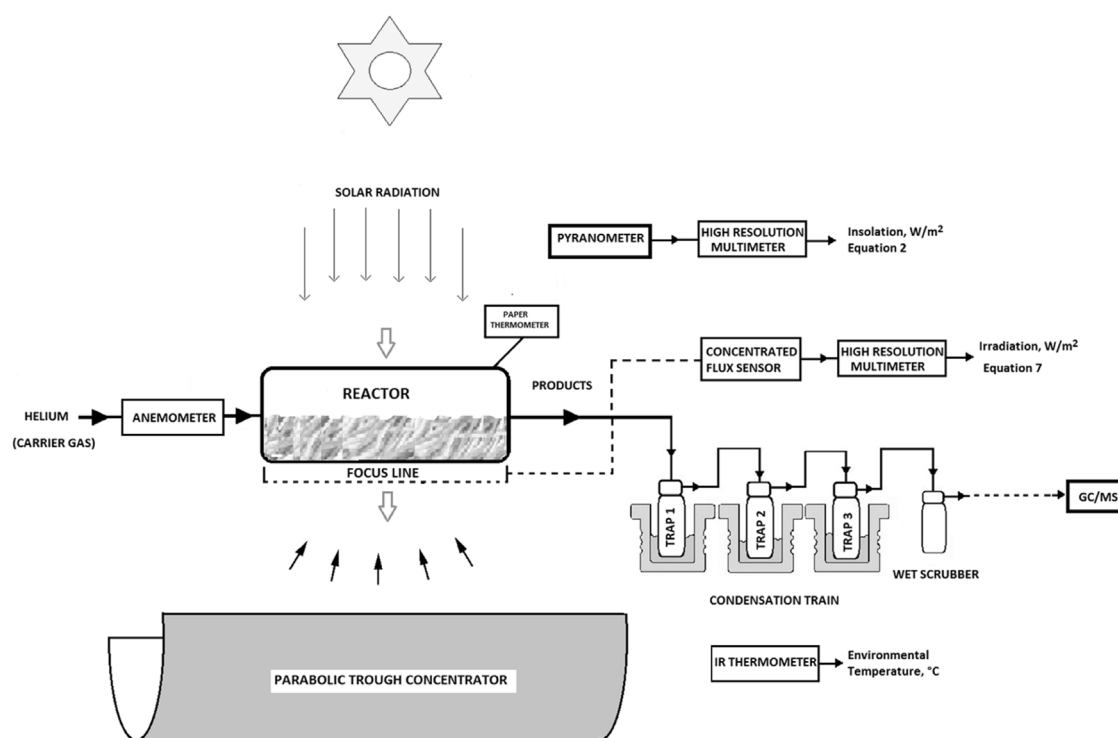


Fig. 2. Schematic diagram of the solar biomass pyrolysis system for the production of bio-fuels.

Table 3

Instrumentation used to monitor and document solar pyrolysis.

Gage	Brand	Model	Variable measured	Units
Pyranometer	Hukseflux	LP02	Insolation	μVDC
Concentrated irradiation sensor	Hukseflux	SG01	Irradiance	μVDC
Anemometer	Fisher Scientific	02-401-5	Gas velocity	m/s
IR Thermometer	NEWPORT	HHM290/N	Environmental temperature	$^{\circ}\text{C}$
High-resolution multimeter	EXTECH	MM570	Linear voltage	μVDC
Paper Thermometer	Paper Thermometer Co., Inc.	TL-8-290	Temperature of the surface of the reactor	$^{\circ}\text{C}$

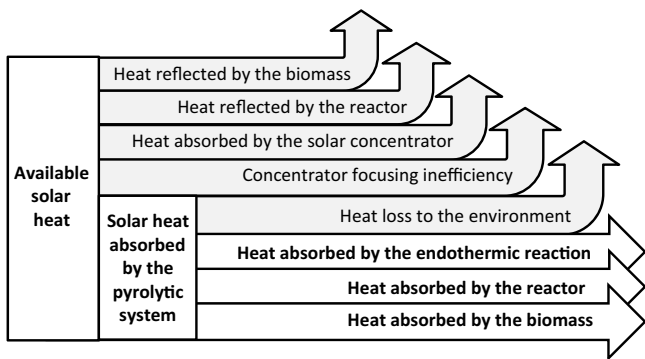


Fig. 3. Heat fluxes and losses involved in the heat balance during solar pyrolysis.

irradiation (q_0) at the middle of the focal line on the surface of the reactor. Both gages had a linear voltage output signal. The linear voltage (V) emitted by the sensors was measured using a high-resolution multimeter and then was converted to energy flux and concentrated irradiation values by correlating the linear voltage with the information reported on the respective calibration sheet for each gage. The anemometer measured the velocity of the gas carrier at the entrance of the reactor. The environmental temperature was measured using an IR thermometer that was pointed at a surface exposed to the environment. The temperature of the reactor surface was determined using two methods, as follows: direct measurement using a paper thermometer with a maximal temperature registration of 143 °C and indirect measurement, by which the temperature was calculated using the method presented in Section 2.8. Table 3 show what gages were used in the present study.

2.6. Characterization of the bio-oil

The pyrolytically produced bio-oil was characterized using an Agilent Model 6890 gas chromatograph coupled to a Model 5973 Network mass spectrometer and a model HP5MS column (30 m × 2 in.), using helium as the carrier gas.

The analytical method employed the following conditions for gas chromatography: an initial oven temperature of 50 °C with a 5-min isothermal period and a subsequent increase of 10 °C/min up to 300 °C, followed by a 10-min isothermal period. The injector temperature was 250 °C and the temperature of the mass spectrometer was 300 °C.

2.7. Mass balance

Three main products were considered in the present biomass pyrolytic study, which were bio-oil, chars and gas products. The bio-oil was collected in the 3 condensation traps. The sum of the weight of the oil in the 3 traps was considered the bio-oil product. The chars, which remained within the reactor, were also weighted and considered the char product. The gas products were calculated by the difference according to Eq. (1), as follows:

$$m_{\text{orange peel}} = m_{\text{bio-oil}}^{\text{trap 1}} + m_{\text{bio-oil}}^{\text{trap 2}} + m_{\text{bio-oil}}^{\text{trap 3}} + m_{\text{chars}} + m_{\text{gas products}} \quad (1)$$

2.8. Heat balance

The thermal performance of the solar system was analyzed by examining the heat balance, which indicated the main sources of energy loss and the areas that could be improved. Fig. 3 shows all of the heat fluxes and losses that occurred during solar pyrolysis in the present study.

The heat balance of the pyrolytic solar system was calculated using Eq. (2), where the main balance was all of the solar energy that

was absorbed by the thermo-solar system ($Q_{\text{absorbed}}^{\text{solar}}$), which was distributed in the three following ways: first, the heat required by the reactor (Q_{reactor}) and the biomass (Q_{biomass}) to reach pyrolytic-reaction conditions; second, the heat lost to the environment ($Q_{\text{loss to environment}}$) and third; the heat of the pyrolytic reactions that were absorbed by the biomass pyrolysis (Q_{rxn}). The solar energy absorbed by the thermo-solar system is the irradiative energy delivered by the solar concentrator to the surface of the reactor (q_0), which was either absorbed by the reactor (α_{reactor}) or by the biomass ($\tau_{\text{reactor}}\alpha_{\text{biomass}}$) [see Eq. (3)]. The biomass was considered to be coated with a liquid intermediary species, as proposed by Boutin et al. [34], and therefore the absorbance of the biomass was expressed as that of these liquid substances.

$$Q_{\text{absorbed}}^{\text{solar}} = Q_{\text{reactor}} + Q_{\text{biomass}} + Q_{\text{loss to environment}} + Q_{\text{rxn}} \quad (2)$$

$$dQ_{\text{absorbed}}^{\text{solar}} = dq_0[\alpha_{\text{reactor}} + \tau_{\text{reactor}}\alpha_{\text{biomass}}] \quad (3)$$

The irradiation on the surface of the reactor was expressed using Eq. (4), as follows

$$dq_0 = \varphi\eta_{\text{optic}}\eta_{\text{focus}}dAdt \quad (4)$$

In which the optical (η_{optic}) and focusing efficiencies (η_{focus}) were considered, as well as the surface area of the reactor (A) and the residence time of the biomass (t).

The distribution of the irradiation along the circumference of the reactor (φ) was expressed using Eq. (5). The irradiation profile across the surface of the reactor depends on the extent of insolation (I) and a fourth-order polynomial function that depends on the circumference of the reactor. This function was based on the data obtained from the optical analysis of the system, which are presented in Section 3.3. Eq. (5) was evaluated using a circumference ranging from −4.326 cm to 4.326 cm, with the origin ($c=0$) located in the middle of the focal line.

$$\varphi = I(2 \times 10^7 c^4 + 2 \times 10^{-10} c^3 - 44828 c^2 - 3 \times 10^{-13} c + 33) \quad (5)$$

where φ is denoted in W/m²; c is denoted in m. Equation created using the results obtained using the Monte Carlo ray-tracing method.

The heat in the reactor (Q_{reactor}) and in the biomass (Q_{biomass}) are the energies required to increase the temperature of these objects from the environmental temperature (T_{∞}) to the operational temperature (T_f). The operational temperature will vary along the circumference of the reactor and the value for the entire system must be acquired by solving all of the heat balance equations. This energy was expressed by the enthalpy that existed during the heating process, as shown in Eqs. (6) and (7), as follows:

$$Q_{\text{reactor}} = M_{\text{reactor}} \int_{T_{\infty}}^{T_f} C_{p_{\text{reactor}}} dT \quad (6)$$

$$Q_{\text{biomass}} = M_{\text{biomass}} \int_{T_{\infty}}^{T_f} C_{p_{\text{biomass}}} dT \quad (7)$$

The heat loss to the environment ($Q_{\text{loss to environment}}$) was expressed by Eq. (8), which depends on the difference between the operational and environmental temperatures, the temperature at the surface of the reactor, and the heat loss coefficient (h) due to convection and radiation phenomena of 2-in. wide horizontal tubes exposed to the environment, which was expressed using, using (Eq. (9), as proposed by Kern [35].

$$dQ_{\text{loss to environment}} = h(T_f - T_{\infty})dAdt \quad (8)$$

$$h = 0.0001T_f^2 + 0.0358T_f + 12.192 \quad (9)$$

where h is donated in W/m² °C; T_f is donated in [°C]. Equation proposed by Kern to express the heat losses occurring due to

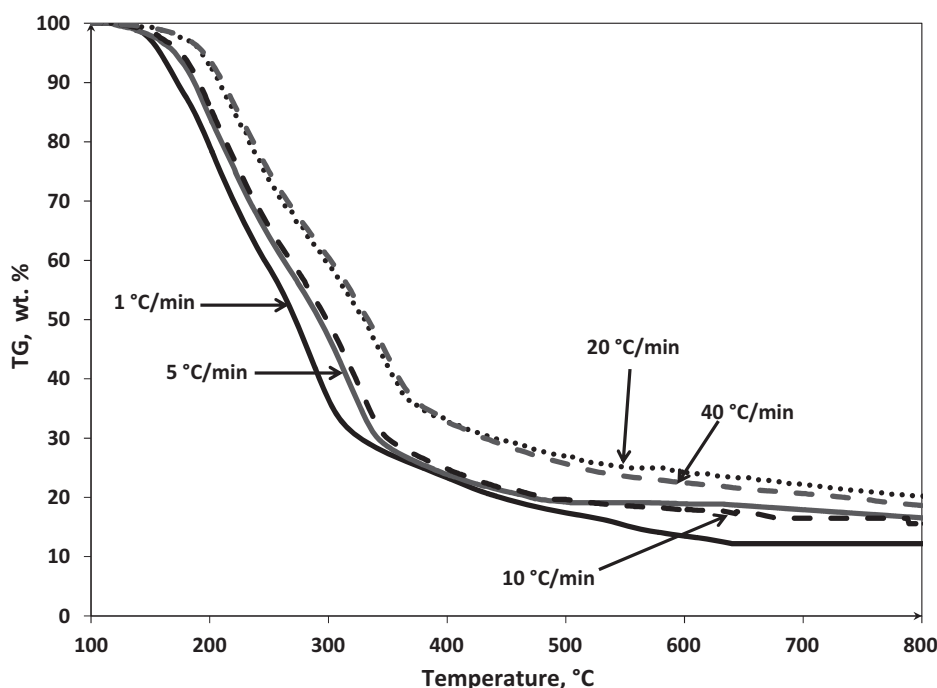


Fig. 4. TG curves of orange peels (dry basis) undergoing thermal decomposition under a N_2 atmosphere that were obtained at heating rates of 1, 5, 10, 20 and 40 °C/min with 450 μm particles. The heating rate increases from left to right.

radiation and convection in horizontal tubes of 2 in. in diameter that are exposed to the environment (Kern [33]).

The reaction heat of pyrolysis (Q_{rxn}) is given by the enthalpy of the pyrolytic reaction of the orange peels (H_{rxn}), expressed using Eq. (10), as follows:

$$Q_{rxn} = H_{rxn}M_{biomass} \quad (10)$$

Table 4 presents all of the constants and parameters needed to solve the system of equations to determine the temperature of the surface of the reactor [Eqs. (3)–(10)].

3. Results and discussion

3.1. Ultimate and proximate analysis

An ultimate analysis of the orange peels was performed. The sample contained 74.79 wt.% volatiles, 13.07 wt.% fixed carbon and 2.94 wt.% ash. Thermochemically processing citrus residues results in a high yield of volatile materials. In addition, the small amount of sulfur (0.6 wt.%) present suggested the production of a bio-fuel with a low sulfur content that would not increase the level of acid-rain precursors upon burning. Table 5 shows results of the ultimate and proximate analyses of different agro-industrial citrus residues.

3.2. Thermogravimetric (TG) analysis

The TG results are presented in Fig. 4, which shows that sample decomposition began when the temperature reached 120 °C and that 85 wt.% of the weight had been lost when the temperature reached 400 °C. Each curve demonstrated 3 stages of weight loss, which can be attributed to the decomposition of different components of the biomass. The first stage occurred between 120 °C and 280 °C, during which 56 wt.% of the weight was lost. The second stage began at 280 °C and ended at approximately 400 °C, when 75 wt.% of the total weight of the sample had been lost. The temperature range of the last stage was 400–800 °C. The final amount of weight loss was 12% at 1 °C/min and 19% at 20 °C/min. A greater amount of

mass was lost at the slowest heating rate (1 °C/min) because a low heating rate allowed the biomass particles to approach the thermochemical equilibrium and therefore, more of the sample was decomposed.

3.3. Optical system analysis

The Monte Carlo ray-tracing method provided a detailed tridimensional description of the optical performance of the thermo-solar system. The focal line was found to be 39 cm from the solar concentrator, and 95.9% of the rays converged at this focal line. The missing rays were either absorbed by the silver coating, which had a 4% rate of absorbance, or were lost due to the specularity of the mirror. Fig. 5 shows the path followed by the solar rays across the system. As the parabolic-trough concentrator was hit by solar rays, they were focused on the surface of the pyrolytic reactor (the 2-in.-diameter tube shown in the middle of Fig. 5). The highest concentration of radiation, that of 33 suns, was found in the middle of the focal line. However, the average irradiance of the reactor surface was 15.65 suns. The parabolic-trough concentrator was therefore able to irradiate as much as 33 times the available solar energy, which was 1 sun.

The irradiance at the surface of the pyrolytic reactor exhibited a Gaussian distribution because the irradiance of the solar disk has the same distribution, as does the parabolically shaped concentrator. In contrast, the irradiance remained nearly constant along the longitudinal axis of the reactor (Fig. 6). The small variation along this axis was due to the specularity of the silver mirror. The Gaussian distribution of irradiance over the surface of the reactor produced a heterogeneous temperature profile along the circumference, with the highest temperature occurring at the center of the focal line and the temperature decreasing with the distance from this position, so that the coldest part of the reactor was located on the opposite side of the tube. Steinfeld et al. [28] reported a similar irradiance profile with a Gaussian distribution over a cylindrical solar collector for air heating, which was irradiated via a parabolic-trough concentrator.

Table 4
Constants and parameters used to analyze heat transfer.

Parameter	Variable	Value	Units	Reference
Absorbance of the biomass	$\alpha_{biomass}$	0.44	Fracc.	Boutin et al. [34]
Absorbance of the reactor	$\alpha_{reactor}$	0.08	Fracc.	Präzisions glas and optik [36]
Diameter of the reactor	Φ	2	in.	Present work
Heat capacity of dried orange peels	$C_p\ biomass$	1244	J/kg°C	Miranda et al. [37]
Environmental temperature during Experiment 1	T_{∞}	28	°C	Present study
Environmental temperature during Experiment 2		30		
Focusing efficiency during Experiment 1	$\eta_{Focusing}$	61.6	%	Present study
Focusing efficiency during Experiment 2		78.9		
Heat capacity of the reactor	$C_p\ reactor$	753	J/kg°C	Präzisions glas and optik [36]
Insolation during Experiment 1	I	827	W/m ²	Present study
Insolation during Experiment 2		965		
Length of reactor	L	0.78	M	Present study
Optical efficiency	η_{optic}	95.9	%	Present study
Reaction enthalpy per mass unit	H_{rxn}	24,480	J/kg	Miranda et al. [37]
Surface area of the reactor	A	0.58	m ²	Present study
Biomass residence time during Experiment 1	t	1230	S	Present study
Biomass residence time during Experiment 2		10,225		
Transmittance of the reactor	$\tau_{reactor}$	0.92	Fracc.	Präzisions glas and optik [36]

Table 5
Results of ultimate and proximate analyses of citrus residues reported in the literature.

Biomass	Component (wt.%)									Reference
	C	H	N	O	S	Moisture	Volatiles	FC	Ash	
Orange peels (<i>Citrus sinensis</i>) ^a	39.71	6.20	0.46	50.09	0.60	9.20	74.79	13.07	2.94	Present Work
Orange waste pulp	47.00	6.90	1.30	44.71	0.09	5.70	74.60	16.68	3.02	Lopez-Velazquez et al. [38]
Orange peels ^a	47.32	5.75	1.39	42.45	0.18	^b	76.49	20.60	2.91	Zhou et al. [39]
Orange embryos (<i>Citrus sinensis</i>)	63.31	9.33	2.54	24.63	0.19	3.83	91.20	1.88	3.09	Hernández-Montoya et al. [40]
Orange husks (<i>Citrus sinensis</i>)	43.32	6.23	0.47	49.79	0.19	9.09	83.91	5.41	1.59	Hernández-Montoya et al. [40]
Lemon seed husks (<i>Citrus limon</i>)	62.22	9.37	4.28	23.87	0.26	5.97	86.45	0.10	2.74	Hernández-Montoya et al. [40]
Lemon seed embryos (<i>Citrus limon</i>)	49.38	6.30	0.47	43.81	0.04	9.42	91.19	3.32	0.81	Hernández-Montoya et al. [40]
Grapefruit seed husks (<i>Citrus paradisi</i>)	63.63	10.65	2.85	22.65	0.22	9.49	84.96	0.00	2.91	Hernández-Montoya et al. [40]
Grapefruit seed embryos (<i>Citrus paradisi</i>)	48.50	6.12	0.30	45.08	0.00	11.23	91.08	3.37	0.44	Hernández-Montoya et al. [40]
Orange peels and seeds	46.40	5.70	1.52	46.33	0.05	7.05	77.11	18.73	4.55	Aguilar et al. [41]

^a The elemental analysis was conducted according to Eq. (1).
^b Not available.

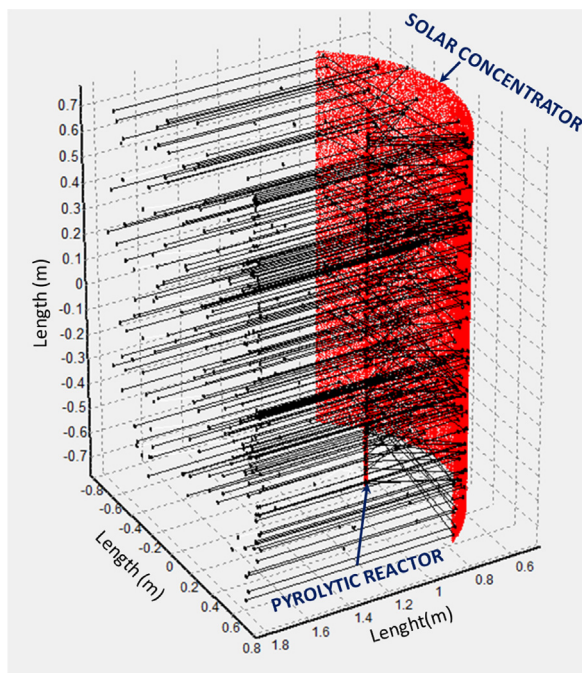


Fig. 5. Path of 200 rays randomly chosen as a sample of those that interacted with the solar concentrator and the pyrolytic reactor. The light rays were traced using SolTrace software.

The actual focal line was experimentally located using a laser scanner. The actual focal line was located 34 cm from the concentrator, which means that was shifted 5 cm from the focal line that was identified using the Monte Carlo ray-tracing method. This difference indicated that the concentrator was manufactured with slight imperfections.

A blank run of the solar pyrolytic reactor was conducted to corroborate the ray-tracing results. During this experiment, the reactor was devoid of biomass. The concentrated irradiance on the surface of the reactor was measured during a day with an insolation of 863 W/m². The maximum irradiance in the middle of the focal line was 27,088 W/m², which represents a concentration of 31.03 times the available solar energy. The experimental thermo-solar system performed at 94% of the optimal level, which was determined using the Monte Carlo ray-tracing method. The 6% level of inefficiency could be attributed to manufacturing imperfections in the concentrator and the inaccurate focusing of the concentrator during operation.

3.4. Solar biomass pyrolysis

Solar pyrolysis of the orange peels (*C. sinensis*) was conducted during a day with an insolation of 965 W/m². The peak irradiance of the solar reactor was 25,084 W/m² and the average irradiance of the reactor was 12,553 W/m². The orange peel sample was directly irradiated trough the wall of the reactor, which was composed of borosilicate glass. The concentrated irradiance allowed the biomass to reach pyrolytic temperatures using only direct solar radiation.

The orange peel sample lost 79.08 wt.% of its mass, and the main product obtained was a bio-oil. The sample shrank during pyrolysis.

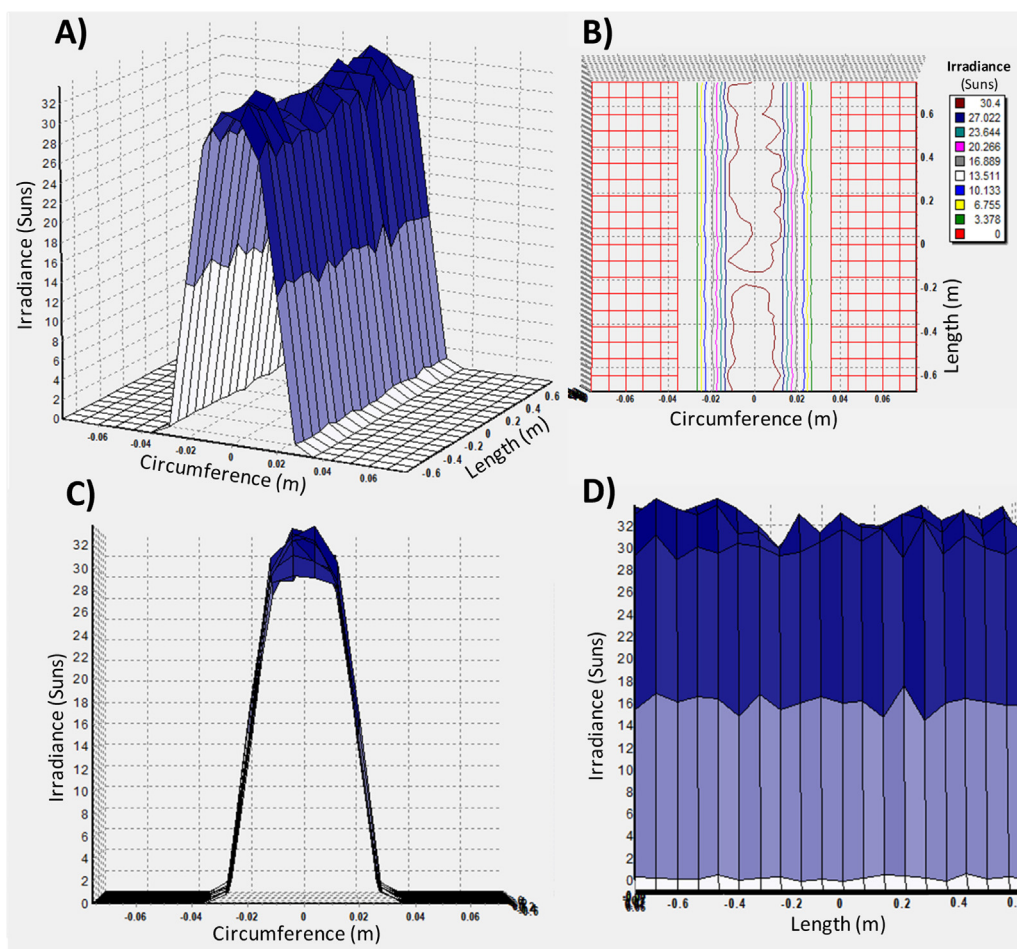


Fig. 6. Monte Carlo ray-tracing method. (A) Tridimensional graph of the distribution of irradiance on the surface of the reactor. (B) Bidimensional graph of the distribution of irradiance on the surface of the reactor. (C) Irradiance distribution along the circumference of the reactor. (D) Irradiance distribution along the longitudinal axis of the reactor.

The yield of the products was as follows: 77.64% liquid, 1.43% bio-gas, and 20.93% char. The mass loss observed in the present study is similar to those reported for citrus peels in the literature and is nearly identical to the value reported by Miranda et al. [37] for the pyrolysis of orange peels using an electric furnace but the yield of bio-oil and biogas are different (Table 6). The differences may be attributed to three causes, included the use of a different heating sources, the use of a reactor with a different geometry or a difference in the temperatures of the condensation traps. During

this study, the three condensation traps were cooled using liquid hydrogen to approximately -200°C , which may have increased the condensation efficiency.

During solar pyrolysis, the reactor reached an average temperature of 290°C , with a peak temperature of 465°C located at the center of the focal line. The total weight loss of the sample was 79.08 wt.%. According to the TG analysis, the orange peel sample reached a weight loss of 60 wt.% at 290°C and 82% at 465°C . The high temperature in the center of the focal line promoted a higher

Table 6

Yields of the products of pyrolysis of different citrus materials.

Raw material	Heating source	Total mass loss (wt.%)	Gas (wt.%)	Char (wt.%)	Oil (wt.%)	Reference
Orange (<i>Citrus sinensis</i>) peels	Sun	79	1.4	21	77.6	Present work
Mandarin residue	Electrical resistance	66	28	34	38	Kim et al. [44]
Orange peel	Electrical resistance	78.9	25.8	21.1	53.1	Miranda et al. [37]
Orange peel	Electrical resistance	63.7	53.2	36.3	10.5	Aguiar et al. [41]
Orange waste ^a	Electrical resistance	77	^b	23	^b	Lopez-Velazquez et al. [38]
Orange peel ^a	Electrical resistance	74	^b	26	^b	Zhou et al. [39]
Orange juice residue ^a	Electrical resistance	76.5	^b	23.5	^b	Virmond et al. [45]
Orange seed husk (<i>Citrus sinensis</i>) ^a	Electrical resistance	81	^b	19	^b	Hernández-Montoya et al. [40]
Orange seed embryo (<i>Citrus sinensis</i>) ^a	Electrical resistance	91	^b	9	^b	Hernández-Montoya et al. [40]
Lemon seed husk (<i>Citrus limon</i>) ^a	Electrical resistance	79	^b	21	^b	Hernández-Montoya et al. [40]
Lemon seed embryo (<i>Citrus limon</i>) ^a	Electrical resistance	89	^b	11	^b	Hernández-Montoya et al. [40]
Grapefruit seed husk (<i>Citrus paradisi</i>) ^a	Electrical resistance	82	^b	18	^b	Hernández-Montoya et al. [40]
Grapefruit seed embryo (<i>Citrus paradisi</i>) ^a	Electrical resistance	88	^b	12	^b	Hernández-Montoya et al. [40]

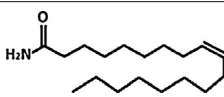
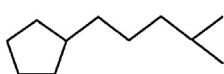
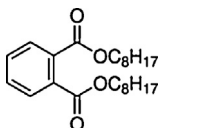
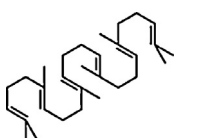

^a Results of thermogravimetric analysis.

^b Not available.

Table 7
Main compounds found in the bio-oil produced by solar pyrolysis of orange peels.

No.	Retention time (min)	Trap	Molecular weight (g/mol)	Compound	Chemical structure
1	0.92	1	58.1	Acetone	
2	0.97	2	207.3	4-[3-(Dimethylamino)propoxy] benzaldehyde	
3	1.49	2	60.1	1,1-Dimethylhydrazine	
4	1.75	2	60.1	1,1-Dimethylhydrazine	
5	3.11	2	96.1	Furfural	
6	7.45	2, 3	94.1	Phenol	
7	8.32	1, 3	136.2	D-Limonene	
8	9.12	2, 3	108.1	2-Methylphenol	
9	9.59	2, 3	108.1	4-Methylphenol	
10	9.73	2	108.1	4-Methylphenol	
11	10.978	2	122.2	2,3-Dimethylphenol	
12	11.33	3	122.2	3-ethylphenol	
14	14.33	3	138.2	(4Z)-cyclonon-4-en-1-one	
15	17.23	1	270.5	Propan-2-yl tetradecanoate	
16	18.56	1	242.4	1-Hexadecanol	$\text{CH}_3(\text{CH}_2)_{14}\text{CH}_2\text{OH}$
17	20.89	1	256.4	Hexyl decanoate	
18	21.11	1	256.4	n-Hexadecanoic acid	
19	24.66	1	310.6	Docosane	$\text{CH}_3(\text{CH}_2)_{20}\text{CH}_3$
20	24.92	1	290.4	Octyl 3-(4-methoxyphenyl)prop-2-enoate	

Table 7 (Continued)

No.	Retention time (min)	Trap	Molecular weight (g/mol)	Compound	Chemical structure
21	25.48	1	281.5	(Z)-9-octadecenamide	
22	26.46	1	350.7	4-Octyldodecylcyclopentane	
23	27.01	1	390.6	Diisooctyl phthalate	
24	29.15	1	410.7	Squalene	
25	29.89	1	236.4	(1S,15S)-Bicyclo[13.1.0]hexadecan-2-one	
26	31.034	1	310.6	Docosane	CH ₃ (CH ₂) ₂₀ CH ₃

rate of decomposition than that expected at the average temperature of the reactor. In addition the occurrence of a photochemical phenomenon should not be discarded.

Various researchers have also reported a higher yield of volatiles from the thermochemical decomposition of various substances subjected to concentrated irradiation compared to the yield obtained in systems using different heating sources, such as electrical resistance and lasers. The cause of this phenomenon is still under debate, and the main theories are the following:

Dellinger et al. [42] proposed that photolysis was induced by radiation at the wavelengths of ultraviolet light and even visible light. The high flux of photons that hit the sample was shown to have photolytic effects in the decomposition of 3,3',4,4'-tetrachlorobiphenyl. The sample was exposed to 95 suns produced by a xenon lamp. To reach a mass loss of 80 wt.%, a temperature of 490 °C had to be reached using concentrated irradiation, in contrast to the 690 °C required when using an electrical-resistance system. Furthermore, the production of tetrachlorodibenzofuran as an intermediary species was also affected, which suggested that the reaction mechanism may have changed.

Lédé [43] observed the same effect for cellulose decomposition upon exposure to concentrated radiation emitted by a xenon lamp. Lédé [43] concluded that the transmittance of biomass particles less than 3 mm in diameter allowed the irradiance to reach the center of the particle and involved a lower resistance to the heat transfer compared to the use of electrical resistance, which heats particles from the outside. This change in the governing heat-transfer phenomenon allows thermochemical decomposition to occur at a lower temperature.

Beattie et al. [19] reported the same increase in the yield of volatiles for solar pyrolysis of coal compared with laser pyrolysis. In this report, the author explained that the Gaussian profile of the irradiance promoted the occurrence of hot spots, which affected the heating-transfer gradients and allowed a higher level of thermal decomposition in those spots. The authors rejected the theory that photolysis is caused by ultraviolet light because the experiments were conducted using a filter to block wavelength of ≤ 350 nm.

Nevertheless, the possibility of photolysis caused by a higher wavelength was not explored.

Tabatabaie-Raissi et al. [16] observed the same phenomenon during the pyrolysis of cellulose subjected to the concentrated radiation of a xenon lamp. They proposed that a self-catalytic phenomenon was produced by the products of pyrolysis. This theory proposed that formic and acetic acids were responsible for this catalysis.

The orange-peel sample lost 79.08 wt.% of its mass during pyrolysis, and the main product obtained was a bio-oil. It was observed that the sample was shrinking during the pyrolysis. The yield of the products obtained was as follows: 77.64% liquid, 1.43% biogas, and 20.93% char. The mass loss observed in the present study is similar to that reported for citrus peels in the literature and is nearly identical to the value reported by Miranda et al. [37] for the pyrolysis of orange peel using an electric furnace, although the yields of bio-oil and biogas differed (Table 6). The different yields may be attributed to three possible causes, including the use of different heating sources, the use of a reactor with a different geometry or a difference in the temperatures of the condensation traps. During the present study, the three condensation traps were cooled with liquid hydrogen to approximately -200 °C, which may have increased the efficiency of condensation.

3.5. Characterization of the bio-oil

Fig. 7 shows the GC–MS spectra of the bio-oil that was collected in the 3 condensation traps. (Z)-9-octadecenamide was identified as the major product of the solar pyrolysis of the orange peels. The main components of the bio-oil are listed in Table 7. There is evidence that (Z)-9-octadecenamide, which is also known as oleamide, can induce sleepiness in animals, such as rats, and in humans. Due to this somniferous effect, oleamide has been studied as a possible treatment for sleep disorders in humans [46–48]. The other useful compounds that were found on the bio-oil were: squalene and D-limonene. Squalene is used as a precursor for the synthesis of steroids [49] and is also used as an adjuvant in vaccines to prevent influenza [50]. D-Limonene is a terpene with a low toxicity

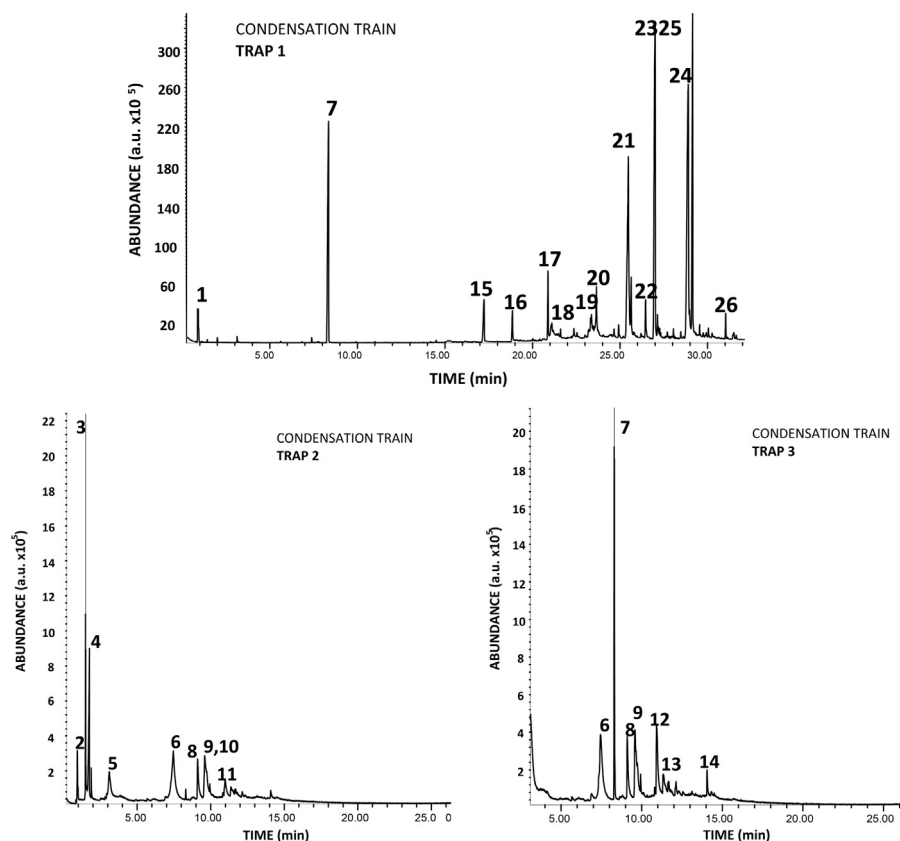


Fig. 7. GC–MS spectra of the orange peel-derived bio-oil found in the 3 traps of the condensation train used in the solar pyrolytic system. The list of compound index can be found in Table 7.

level that is used by the food industry as a flavoring and by the pharmaceutical industry to produce treatments for biliary lithiasis; some studies have investigated over its therapeutic effects against breast and colon cancer [51]. The components in the bio-oil raise the possibility of using solar biomass pyrolysis for the production of a sustainable liquid fuel and of other commodities valuable to the pharmaceutical and chemical industries.

Table 7 Main compounds found in the bio-oil produced by solar pyrolysis of orange peels. The nitrogen-containing substances, such as 1,1-dimethylhydrazine and (Z)-9-octadecenamide were produced as a result of the nitrogen content of the biomass. Amides were produced during pyrolysis of carbonaceous material that included proteins, which contain nitrogen [52–54]. If the entire reactor was at a pyrolytic temperature, the amides would be decomposed while in the gas phase into HCN, NH₃ and HNCO and would become part of the incondensable biogas [52,55]. In the present study, the pyrolytic temperatures occurred only in the lower part of the reactor that was in direct contact with the concentrated solar radiation, so decomposition of amides in the gas phase did not occur because these compounds immediately reached a cooler zone of the reactor. L     [43] reported observing this same effect for the products of pyrolysis due to the heterogeneity of the temperature around the reactor and proposed using a radiative heat source to study chemical substances that generally decompose when other heating methods are used.

3.6. Heat balance

The equation system [Eq. (3)–(10)] was solved using the experimental data that was gathered during solar pyrolysis of the orange peels.

The temperature profile of the surface of the reactor was calculated using the irradiance profile determined using the Monte Carlo ray-tracing method. Fig. 8 shows the temperature profile along the circumference of the reactor that was observed in experiments 1 and 2. The origin of the abscise axis represents the point of the reactor point located in the center of the focal line. This point reached the highest temperature and received the greatest irradiance. The average temperature at the surface of the reactor during Experiment 2 was 290 °C, which is a pyrolytic temperature for orange peels, although, the temperature at the center of the focal

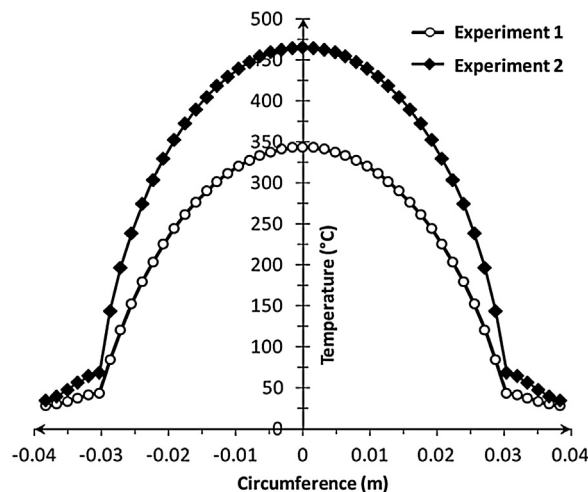


Fig. 8. Temperature profile along the circumference of the reactor. The origin of the abscise axis represents the center of the focal line.

Table 8

Performance of different parabolic-trough solar collectors.

Brand	Model	Production scale	Aperture width (m)	Temperature (°C)	Reference
UNAM	PTC-90	Prototype	1.06	108	Jaramillo et al. [55]
AEE INTEC	Parasol	Prototype	0.5	200	Fernandez-Garcia et al. [11]
Soliterm	PTC 1000	Prototype	1	200	Fernandez-Garcia et al. [11]
UANL	PROMETEO 01	Prototype	1.3	290	Present Work
Solel Solar Systems	IND-300	Industrial	1.3	300	Fernandez-Garcia et al. [11]
Acurex Corp.	3001	Industrial	1.83	320	Fernandez-Garcia et al. [11]
Acurex Corp.	3011	Industrial	2.13	320	Fernandez-Garcia et al. [11]
Solar Kinetics Inc.	T-700	Industrial	2.13	350	Fernandez-Garcia et al. [11]
Instituto de Investigaciones Eléctricas	IIE	Prototype	2.3	400	Fernandez-Garcia et al. [11]
Solar Kinetics Inc.	T-800	Industrial	2.36	320	Fernandez-Garcia et al. [11]
Luz International Ltd.	LS-1	Industrial	2.5	307	Fernandez-Garcia et al. [11]
Suntec Systems Inc.	IV	Industrial	3.05	320	Fernandez-Garcia et al. [11]
Luz International Ltd.	LS-2	Industrial	5	349	Fernandez-Garcia et al. [11]
Luz International Ltd.	LS-3	Industrial	5.76	390	Fernandez-Garcia et al. [11]
Eurotrough Consortium	ET-100	Industrial	5.76	390	Zarza et al. [56]
Indian Institute of Technology Madras	^a	Simulation	6	400	Reddy and Ravi Kumar [57]
LPTPM	^a	Simulation	5	527	Ouagued et al. [58]
ETH Zurich	^a	Simulation	9.5	601	Bader et al. [59]

^a Present study. The solar concentrator was designed and built at the Universidad Autónoma de Nuevo León.

line reached 465 °C. During Experiment 1, the surface of the reactor had an average temperature of 203 °C and the peak temperature was 343 °C at the center of the focal line. The difference in temperatures was caused by the different amounts of solar radiation available when the experiments were performed and the differences in the accuracy of focusing the solar concentrator during the procedures.

The temperature profile suggested a more rapid shrinking of the biomass at the focal line, which due to gravity helped the rest of the biomass located in colder areas to reach a hotter zone in the reactor, thus favoring the thermochemical decomposition of the biomass. Table 8 shows the operational temperatures of different parabolic-trough concentrators. As the aperture length increased, the operational temperature also increased. The average operational temperature in the present study (290 °C) was very similar to that reported for the Solel Solar System model IND-300 (300 °C), which had the same aperture length (1.3 m) [11]. Should a higher operational temperature be required, a concentrator with a longer aperture could be used, such as the LS-3, which is 5.67-m long and reaches to 390 °C.

Table 8 Performance of different parabolic-trough solar collectors. Heat loss and energy balance analyses of the solar pyrolysis process were performed (Table 9). These analyses indicated parts of the process that could be improved in the future. The main heat losses appeared to be due to the reflectivity of the biomass (37.85%) and the difference between the temperatures of the environment and the reactor (36.23%). The difference between the absorptivity of the biomass and that of a black body caused irradiation to be reflected and therefore heat loss. In other words, the biomass absorbed only a percentage of the incoming irradiance. Improving this intrinsic factor of the biomass is a great challenge; nevertheless, Boutin et al. [17] reported improving the absorbance of cellulose during flash pyrolysis produced by the concentrated irradiation of

a xenon lamp by mixing the raw material with coal. Such a change in the composition of the raw material will also affect the chemical composition of the products. The heat loss to the environment was due to the pyrolytic reactor lacking insulation.

Heat loss also occurred as a result of the inaccurate focusing of the concentrator during the operation. The optical loss in the silver mirror was 4.1% because the silver mirror was a high-efficiency reflecting surface. Finally, 0.72% of the energy was absorbed by the endothermic reactions of orange-peel pyrolysis. The majority of the available energy was used to reach and maintain the operational temperature, not used as the input energy required by the endothermic nature of the biomass pyrolysis.

4. Conclusions

A parabolic-trough solar collector was designed and constructed to produce a bio-fuel through biomass pyrolysis. The solar biomass pyrolytic process offers an interesting opportunity for the storage and transportation of solar energy. The experimental solar irradiation peak was 27,088 W/m², which represents a concentration of 31.03 times the available solar energy. The highest concentration of radiation found in the middle of the focal line using the ray tracing method was similar to the solar irradiation of the solar reactor. The temperature reached in the focal line of the reactor was 465 °C. The absorbed portion of the concentrated solar radiation triggered endothermic chemical reactions that produced chemical fuels.

When orange peel samples were pyrolyzed in an inert atmosphere at 1 atm of pressure through direct absorption of concentrated solar radiation at an average flux level of 12,553 W/m², approximately 79 wt.% of the sample was volatilized. The solar pyrolysis reactor used in this study was capable of pyrolyzing the biomass to a liquid (77.64 wt.%) and a non-condensable gas (1.43 wt.%), leaving 20.93 wt.% char in the reactor. The condensable gases were removed from the hot zone by the carrier gas before the liquid products were decomposed into less valuable gaseous products.

Monterrey, Mexico has favorable climatic conditions for the use of solar energy. The city receives approximately 2245 kWh/m²a of solar energy, which would provide the energy to drive thermo solar conversion processes, as reported by Morales et al. [29].

Two different ranges of particle size were tested. The results showed that the final conversion rate was increased when particle size was decreased because the surface area of the solid increased when particle size decreased. The main compounds obtained by solar pyrolysis of orange peels were terpenes, amides and alkanes.

Table 9

Heat balance of solar biomass pyrolysis during Experiment 2.

Parameter	Energy distribution	
	Heat (kJ)	Percentage (%)
Available solar heat	5130.78	100.00
Heat loss due to optic inefficiency	210.36	4.10
Heat loss due to focusing inaccuracy	1082.49	21.10
Heat loss due to biomass reflectivity	1941.99	37.85
Heat loss to the environment	1858.95	36.23
Energy absorbed by the endothermic reactions	36.94	0.72

Solar pyrolytic processes could become important methods for producing solar liquids fuels because of their potential for converting unlimited amounts of solar energy into chemical energy. Additionally, replacing other processes with solar pyrolytic processes would reduce harmful emissions and help mitigate greenhouse gases.

Acknowledgments

The authors are grateful to the investigators at the Plataforma Solar de Almería (PSA) and the National Renewable Energy Laboratory (NREL). This study was financed by the University of Nuevo León (Universidad Autónoma de Nuevo León) and the Mexican government through CONACYT (Consejo Nacional para la Ciencia y Tecnología).

References

- [1] B. Crossette, Estado de la Población Mundial 2011, 1st ed., Fondo de Población de las Naciones Unidas, New York, 2011.
- [2] P. Basu, Biomass Gasification and Pyrolysis Practical Design, 1st ed., Academic Press, Kidlington, Oxford, 2010.
- [3] N.R. Singh, W.N. Delgass, F.H. Ribeiro, R. Agrawal, Estimation of liquid fuel yields from biomass, *Environ. Sci. Technol.* 44 (2010) 5298–5305.
- [4] M. Ringer, V. Putsche, J. Scahill, Large-scale Pyrolysis Oil Production: A Technology Assessment and Economic Analysis, NREL, Colorado, 2006.
- [5] E.G. Hertwich, X. Zhang, Concentrating-solar biomass gasification process for a 3rd generation bio-fuel, *Environ. Sci. Technol.* 43 (2009) 4207–4212.
- [6] A. Nzihou, G. Flamant, B. Stanmore, Synthetic fuels from biomass using concentrated solar energy – a review, *J. Energy* 42 (2012) 121–131.
- [7] M. Pfänder, E. Lüpfer, P. Heller, Pyrometric temperature measurements on solar thermal high temperature receivers, *J. Sol. Energy – T ASME* 128 (2006) 285–292.
- [8] A. Luzzi, K. Lovegrove, Solar Thermal Power Generation, Australian National University, Canberra, 2004, pp. 669–683.
- [9] A. Leitner, Fuel from the Sky, 1st ed., NREL, USA, 2002.
- [10] R. Adinberg, M. Epstein, J. Karni, Solar Gasification of biomass: a molten salt pyrolysis study, *J. Sol. Energy – T ASME* 126 (2004) 586–590.
- [11] A. Fernandez-Garcia, E. Zarza, L. Valenzuela, M. Pérez, Parabolic-trough solar collectors and their applications, *Renew. Sustain. Energy Rev.* 14 (2010) 1695–1721.
- [12] Y. Xuan, X. Chen, Y. Han, Design and analysis of solar thermophotovoltaic systems, *Renew. Energy* 36 (2011) 374–387.
- [13] L. Guiqiang, P. Gang, S. Yuehong, J. Jie, S.B. Riffat, Experiment and simulation study on the flux distribution of lens-walled compound parabolic concentrator compared with mirror compound parabolic concentrator, *Energy* 58 (2013) 398–403.
- [14] N. Velázquez, O. García-Valladares, D. Saucedo, R. Beltrán, Numerical simulation of a Linear Fresnel Reflector Concentrator used as direct generator in a Solar-GAX cycle, *Energy Convers. Manag.* 51 (2010) 434–445.
- [15] M. Randle, Nutzung von Solarenergie mit Linearen Fresnellinsen, Hochschule Mannheim, Germany, 2007, pp. 126–135.
- [16] A. Tabatabaie-raissi, W.S.L. Mok, M.J. Antal, Cellulose pyrolysis kinetics in a simulated solar environment, *Ind. Eng. Chem. Res.* 28 (1989) 565–586.
- [17] O. Boutin, M. Ferrer, J. Lédé, Flash pyrolysis of cellulose pellets submitted to a concentrated radiation: experiments and modelling, *Chem. Eng. Sci.* 57 (2002) 15–25.
- [18] O. Boutin, M. Ferrer, J. Lédé, Radiant flash pyrolysis of cellulose – evidence for the formation of short life time intermediate liquid species, *J. Anal. Appl. Pyrolysis* 47 (1998) 13–31.
- [19] W. Beattie, R. Berjoan, J. Coutures, High-temperature solar pyrolysis of coal, *Sol. Energy* 31 (1983) 137–143.
- [20] K. Imazaki, Biomass Energy Conversion Apparatus, Japanese Patent JP 2010030870 (2010).
- [21] N. Ugolin, Method Using Solar Energy, Microwaves and Plasmas to Produce a Liquid Fuel and Hydrogen from Biomass or Fossil Coal, US Patent. US 8388706 (2010).
- [22] N. Limon-Vazquez, F. Chavez-Lara, Collector and Systems for Generating Steam from the Use of Solar Energy, Mexican Patent MX 2010012078 (2012).
- [23] B.L. Storey, J.P. Monceaux, Extracting Energy Products from Biomass Using Solar Energy, British Patent GB 2458529 (2009).
- [24] F.M. Warzel, Apparatus for Solar Retorting of Oil Shale, US Patent US 4588478 (1986).
- [25] R. E. Mcalister, Carbon Recycling and Reinvestment Using Thermochemical Regeneration, European Patent EP 2534228 (2012).
- [26] A. Weimer, E. Dahl, J.R. Pitts, A.A. Lewndowski, C. Bingham, J.R. Tamburini, Solar Thermal Aerosol Reaction Process, US Patent US 6872378 (2003).
- [27] J. Lédé, Thermochemical conversion of biomass, *Sol. Energy* 65 (1998) 3–13.
- [28] A. Steinfeld, A.W. Weimer, Thermochemical production of fuels with concentrated solar energy, *J. Opt. Soc. Am. A* 18 (2010) A100–A111.
- [29] S. Morales, R. Miranda, E. Ramírez-Lara, J.D.W. Kahl, H. Tran, Impact of Typical Solar Radiation, Temperature and Relative Humidity on Photochemical Pollutants Concentration in Northeastern Mexico, *Atmosfera*, 2014.
- [30] V. Ferreira-Leitao, L.M. Fortes Gottschalk, M.A. Ferrara, A. Lima Nepomuceno, H.B. Correa Molinari, E.P.S. Bon, Biomass residues in Brazil: availability and potential uses, *Waste Biomass Valoriz.* 1 (2010) 65–76.
- [31] FAOSTAT, Food and Agricultural Commodities Production, Statistical Database, 2010 <http://faostat.fao.org/site/339/default.aspx> (accessed July 2012).
- [32] R. Miranda Guardiola, S. Morales Valdes, C.A. Sosa Blanco, D. Bustos Martinez, Ma. E. Rodriguez Cantu, Proceso para la Producción de Bioaceite, Biocombustible, Biogas y Carbon a partir de Pirólisis Solar de Biomasa, Mexican Patent MX 2012014867 (2012).
- [33] S. Morales Valdés, Proceso para la Producción de un Biocombustible de Tercera Generación, Bioaceite, Biogas y Carbón a partir de una Pirólisis Solar, Universidad Autónoma de Nuevo León Mexico, 2012.
- [34] O. Boutin, J. Lédé, G. Olalde, A. Ferrier, Solar flash pyrolysis of biomass direct measurement of the optical properties of biomass components, *J. Phys. IV France* 9 (1999) 369–372.
- [35] D. Kern, Process Heat Transfer, 31st ed., MacGraw Hill, USA, 1999.
- [36] Präzisions glas, optik, Thermal Glass. Block-Rolled Glass, 2011 <http://www.pgo-online.com/intl/katalog/pyrex.html> (accessed 21.11.11).
- [37] R. Miranda, D. Bustos-Martínez, C. Sosa Blanco, M.H. Gutiérrez Villarreal, M.E. Rodríguez Cantú, Pyrolysis of sweet orange (*Citrus sinensis*) dry peel, *J. Anal. Appl. Pyrolysis* 86 (2009) 245–251.
- [38] M.A. Lopez-Velazquez, V. Santosa, J. Balmaseda, E. Torres-Garcia, Pyrolysis of orange waste: a thermo-kinetic study, *J. Anal. Appl. Pyrolysis* 99 (2013) 170–177.
- [39] H. Zhou, Y. Long, A. Meng, Q. Li, Y. Zhang, The pyrolysis simulation of five biomass species by hemi-cellulose, cellulose and lignin based on thermogravimetric curves, *Thermochim. Acta* 566 (2013) 36–43.
- [40] V. Hernández-Montoya, M.A. Montes-Morán, M.P. Elizalde-González, Study of the thermal degradation of citrus seeds, *Biomass Bioenergy* 33 (2009) 1295–1299.
- [41] L. Aguiar, F. Marquez-Montesinos, A. Gonzalo, J.L. Sánchez, J. Arauzo, Influence of temperature and particle size on the fixed bed pyrolysis of orange peel residues, *J. Anal. Appl. Pyrolysis* 83 (2008) 124–130.
- [42] B. Dellinger, J. Graham, J.M. Bernam, D. Klosterman, High Temperature photochemistry induced by concentrated solar radiation, in: Workshop on Potential Applications of Concentrated Solar Photons, NRC, Colorado, 1990.
- [43] J. Lédé, Comparison of contact and radiant ablative pyrolysis of biomass, *J. Anal. Appl. Pyrolysis* 70 (2003) 601–618.
- [44] J.W. Kim, S.H. Park, J. Jung, J. Jeon, C.H. Ko, K. Jeong, Y. Park, Catalytic pyrolysis of mandarin residue from the mandarin juice processing industry, *Bioresour. Technol.* 136 (2013) 431–436.
- [45] E. Virmond, R.F. De Sena, W. Albrecht, C.A. Althoff, R.F.P.M. Moreira, H.J. José, Characterisation of agroindustrial solid residues as bio-fuels and potential application in thermochemical processes, *Waste Manag.* 32 (2012) 1952–1961.
- [46] S. Huitron-Resendiz, L. Gombart, B.F. Cravatt, S.J. Henriksen, Effect of oleamide on sleep and its relationship to blood pressure, body temperature and locomotor activity in rats, *Exp. Neurol.* 172 (1) (2001) 235–243.
- [47] I. Fedorova, A. Hashimoto, R.A. Fecik, Behavioral evidence for the interaction of oleamide with multiple neurotransmitter system, *J. Pharmacol. Exp. Ther.* 299 (1) (2001) 332–342.
- [48] B.F. Cravatt, O. Prospero-Gracia, G. Siuzdak, N.B. Gilula, S.J. Henriksen, D.L. Boger, R.A. Lerner, Chemical characterization of a family of brain lipids that induce sleep, *Science* 268 (5216) (1995) 1506–1509.
- [49] B.E. Konrad, Sterol, structure and membrane function, *Crit. Rev. Biochem. Mol. Biol.* 14 (1983) 47–92.
- [50] World Health Organization, Squalene-based adjuvants in vaccines, Global Advisory Committee on Vaccine Safety, 2008 http://www.who.int/vaccine-safety/committee/topics/adjuvants/squalene/questions_and_answers/en/ (accessed 30.01.12).
- [51] J. Sun, D-Limonene: safety and clinical applications, *Altern. Med. Rev.* 12 (3) (2007) 259–264.
- [52] K.M. Hannson, J. Samuelsson, C. Tullin, L.E. Amand, Formation of HNCO, HCN NH₃ from the pyrolysis of bark and nitrogen-containing model compounds, *Combust. Flame* 137 (2004) 265–277.
- [53] C. Di Blasi, Modeling chemical and physical processes of wood and biomass pyrolysis, *Prog. Energy Combust. Sci.* 34 (2008) 47–90.
- [54] I. Fonts, M. Azuara, G. Gea, M.B. Murilo, Study of the pyrolysis liquids obtained from different sewage sludge, *J. Anal. Appl. Pyrolysis* 85 (2009) 184–191.
- [55] O.A. Jaramillo, E. Venegas-Reyes, J.O. Aguilar, R. Castrejón-García, F. Sosa-Montemayor, Parabolic trough concentrators for low enthalpy processes, *Renew. Energy* 60 (2013) 529–539.
- [56] E. Zarza, E. Ma, L. Rojas, J. González, Ma. Caballero, F. Rueda, INDITEP: the first pre-commercial DSG solar power plant, *Sol. Energy* 80 (2006) 1270–1276.
- [57] K.S. Reddy, K. Ravi Kumar, Solar collector field design and viability analysis of stand-alone parabolic trough power plants for Indian conditions, *Energy Sustain. Dev.* 16 (2012) 456–470.
- [58] M. Ouagued, A. Khellaf, L. Loukarfi, Estimation of the temperature, heat gain and heat loss by solar parabolic trough collector under Algerian climate using different thermal oils, *Energy Convers. Manag.* 75 (2013) 191–201.
- [59] R. Bader, M. Barbato, A. Pedretti, A. Steinfeld, An air-based cavity-receiver for solar trough concentrators, *J. Sol. Energy Eng.* 132 (3) (2010), 031017 1–7.